

A quantum chemical study of repair of O6-methylguanine to guanine by tyrosine: Evaluation of the winged helix-turn-helix model

Saumya Tiwari · Phool Chand Mishra

Received: 13 January 2009 / Accepted: 16 April 2009 / Published online: 7 May 2009
© Springer-Verlag 2009

Abstract The winged helix-turn-helix model for the repair of O6-MeG to guanine involving the reaction of O6-MeG with a tyrosine residue of the protein O6-alkylguanine-DNA alkyltransferase (AGT) was examined by studying the reaction mechanism and barrier energies. Molecular geometries of the species and complexes involved in the reaction, i.e. the reactant, intermediate and product complexes as well as transition states, were optimized employing density functional theory in gas phase. It was followed by single point energy calculations using density functional theory along with a higher basis set and second order Møller-Plesset perturbation theory (MP2) along with two different basis sets in gas phase and aqueous media. For the solvation calculations in aqueous media, the integral equation formalism of the polarizable continuum model (IEF-PCM) was employed. Vibrational frequency analysis was performed for each optimized structure and genuineness of transition states was ensured by visualizing the vibrational modes. It is found that tyrosine can repair O6-MeG to guanine by a two-step reaction. The present results have been compared with those obtained considering the helix-turn-helix model where the repair reaction primarily involves cysteine and occurs in a single-step. It is concluded that the repair through tyrosine envisaged in the winged helix-turn-helix model would be less efficient than that through cysteine envisaged in the helix-turn-helix model.

Keywords Cancer · DNA damage · DNA repair · O6-methylguanine · Mutation · Winged helix-turn-helix model

S. Tiwari · P. Chand Mishra (✉)
Department of Physics, Banaras Hindu University,
Varanasi 221 005, India
e-mail: pcmishra_in@yahoo.com

Introduction

Many cellular and environmental agents continuously attack DNA in cells, causing a variety of damage to it [1–5]. The DNA damage sources can be subdivided into two main types, i.e. exogenous and endogenous. The exogenous sources include chemical pollutants, UV radiation, e.g. that from the sun, chemotherapy and radiotherapy while the endogenous sources include the normal metabolic byproducts, e.g. the OH radical, ONOO[−] (peroxynitrite), H₂O₂ etc. [6–8]. The agents that cause damage to DNA are also classified as reactive oxygen species (ROS), reactive nitrogen oxide species (RNOS) and alkylating agents. Such damages can be prevented by the action of anti-oxidants [9]. DNA damage gives rise to aging, chronic inflammatory diseases, mutation, cancer and neurodegenerative disorders such as the Alzheimer's and Parkinson's diseases [10–13].

Methylating agents are widespread in the biological environment and can cause a broad spectrum of DNA damage [4, 5, 14–16]. Alkyl-DNA lesions can arise from endogenous sources such as S-adenosylmethionine [17] and N-methyl-N-nitro-N-nitrosoguanidine (MNNG) [18]. Reactions of alkylating agents with the DNA bases produce many different adducts that can alter DNA properties [5, 14]. Among these, addition of alkyl groups at the O6 position of guanine is of major importance. Formation of O6-methylguanine (O6-MeG) can result in G:C to A:T transversion mutation during replication which is both mutagenic and cytotoxic [19, 20]. Thus formation of the O6-MeG lesions is of considerable interest from the point of view of mutation and cancer [21–23].

The mechanism of repair of O6-MeG to guanine involves action of the protein O6-alkylguanine-DNA alkyltransferase (AGT), also known as O6-methylguanine-DNA methyltransferase (MGMT). Wetmore and coworkers

[24–26] have studied stacking interactions between the aromatic amino acids and the natural or methylated nucleobases and concluded that strengthening of the stacking interactions upon methylation helps selective removal of the alkylated bases over the natural bases. AGT is a natural defense system against DNA damage and removes numerous alkyl groups from the O6 position of guanine [27, 28]. The presence of AGT is known to protect cells from alkylating agent-mediated toxicity including mutagenesis, cell killing and carcinogenesis [29]. However, the presence of AGT in tumors also provides resistance to therapeutic alkylating agents [30]. Another type of DNA lesion known to be repaired by AGT is O4-methylthymine. However, the extent of repair of O4-methylthymine to thymine by AGT is very low [31].

Properties of the DNA bases and base pairs have been extensively studied [32, 33]. The molecular mechanism of the repair action of AGT has also been a subject of intense research. Two models have been proposed in this context. One of them due to Daniels *et al.* [34] based on the crystal structure of AGT bound to DNA is called helix-turn-helix (HTH) model. According to this model [34], AGT flips the alkylated base to be repaired out of the stack of the DNA bases that gets bound to the active site of AGT. In this model, a cysteine residue (Cys145) receives the alkyl group removed from the O6 site of guanine. The reaction mechanism of DNA repair by AGT has been studied theoretically according to the HTH model using density functional theory [35].

The second model for the binding of AGT to a DNA substrate and repair of O6-MeG to guanine known as winged helix-turn-helix (WHTH) model was proposed by Goodtzova *et al* [36]. In this model, a tyrosine residue (Tyr114) plays the main role in both DNA binding and alkyl group transfer from O6-MeG. There is no theoretical study reported so far on the repair of O6-MeG to guanine according to this model. In the present work, we have studied the mechanism of repair of O6-MeG to guanine by tyrosine considering this model.

Computational details

Molecular geometries of the *cis* and *trans* isomers of O6-MeG and those of three most stable conformers of tyrosine (I, II and III) were fully optimized using density functional theory at the B3LYP/6-31G(d,p) level in gas phase [37–39]. Geometries of reactant complexes (RCs), intermediate complex (IC1), transition states (TSs) and product complexes (PCs) involved in the reaction of O6-MeG with tyrosine as well as with phenol were also optimized at the B3LYP/6-31G(d,p) level of theory in gas phase. Single point energy calculations for all the optimized species and

complexes were performed at the B3LYP/AUG-cc-pVDZ and MP2/AUG-cc-pVDZ levels of theory [40–42] in gas phase. Ideally, a few specific water molecules placed at appropriate positions should be included in the treatment of the solvent effect and also geometry optimization should be performed in bulk aqueous media. However, in the present work, solvent effect was treated approximately by solvating B3LYP/6-31G(d,p) level gas phase optimized structures in bulk aqueous media using single point energy calculations at the B3LYP/6-31G(d,p), B3LYP/AUG-cc-pVDZ and MP2/AUG-cc-pVDZ levels of theory and the integral equation formalism of the polarizable continuum model (IEF-PCM) [43–46]. Electrostatic potential-fitted model charges located at the atomic sites were obtained using the CHelpG algorithm [47] at the MP2/AUG-cc-pVDZ level of theory in aqueous media.

Vibrational frequency analysis was performed for each optimized structure at the B3LYP/6-31G(d,p) level of theory in gas phase in order to ensure that each searched total energy extremum was genuine, each minimum having all real vibrational frequencies and each transition state having only one imaginary frequency. Genuineness of transition states was ensured by visually examining the vibrational modes corresponding to the imaginary frequencies and applying the condition that these connected the reactant and product complexes properly. As genuineness of the optimized transition states was obvious, intrinsic reaction coordinate (IRC) calculations were not performed for this purpose. Gibbs free energies at 298.15 K and zero-point energy (ZPE)-corrected total energies were obtained in each case at the B3LYP/6-31G(d,p) level of theory in gas phase. As an approximation, the ZPE corrections and thermal energy corrections giving Gibbs free energies obtained at the B3LYP/6-31G(d,p) level were also applied to the total energies obtained by single point energy calculations at all the other levels of theory employed here in both gas phase and aqueous media. All the calculations were carried out using the Windows version of the Gaussian98 (G98W) [48] program. For visualization of the optimized structures and vibrational modes, the Gauss-View program was employed [49].

Results and discussion

Structure and stability

Structures of *cis* and *trans* isomers of O6-MeG and those of three conformers of tyrosine (I, II, III) obtained by geometry optimization at the B3LYP/6-31G(d,p) level in gas phase along with the corresponding ZPE-corrected relative total energies obtained at the MP2/AUG-cc-pVDZ level in aqueous media are presented in Fig. 1. The ZPE-

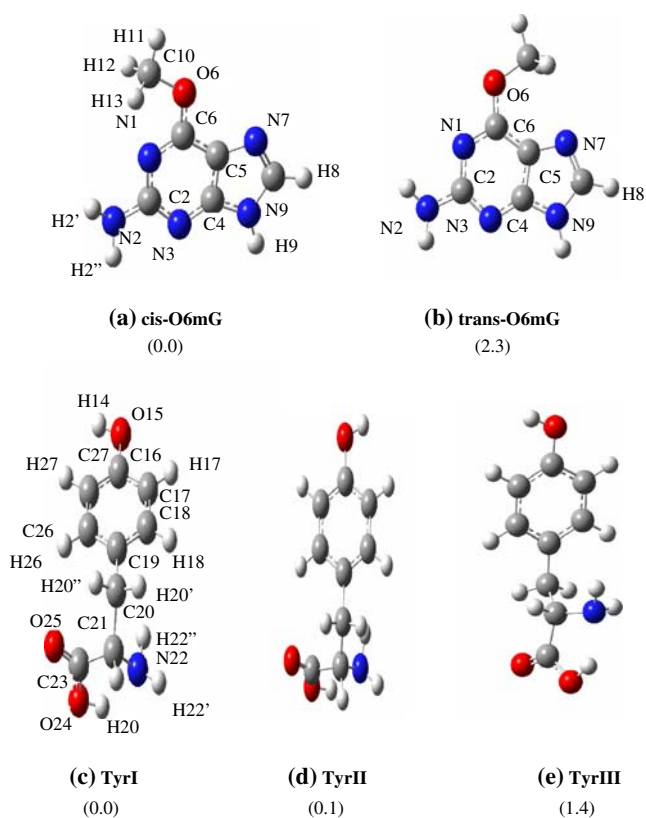


Fig. 1 Two (*cis* and *trans*) conformers of O6-MeG (a, b) and three (TyrI, TyrII and TyrIII) conformers of tyrosine (c, d, e). Relative ZPE-corrected total energies (kcal mol^{-1}) of (a) and (b) obtained in aqueous media at the MP2/AUG-cc-pVDZ level of theory using the geometries optimized at the B3LYP/6-31G(d,p) level in gas phase are given with respect to that of (a). Relative ZPE-corrected total energies (kcal mol^{-1}) of (c), (d) and (e) obtained in aqueous media at the MP2/AUG-cc-pVDZ level of theory using the geometries optimized at the B3LYP/6-31G(d,p) level in gas phase are given with respect to that of (c)

corrected total energies in aqueous media show that the *cis* conformer of O6-MeG (defined with respect to the N1C6O6C10 dihedral angle) is more stable than the *trans* conformer at the MP2/AUG-cc-pVDZ level of theory by $2.3 \text{ kcal mol}^{-1}$ while the corresponding Gibbs energy difference is $2.2 \text{ kcal mol}^{-1}$. Previous X-ray crystallographic and low level *ab initio* quantum chemical studies have also shown that *cis* O6-MeG is more stable than *trans* O6-MeG [50, 51]. The ZPE-corrected total energies in aqueous media obtained at the MP2/AUG-cc-pVDZ level of theory show that the II and III conformers of tyrosine are less stable than the I conformer by 0.1 and $1.4 \text{ kcal mol}^{-1}$ respectively. Thus the conformers I and II of tyrosine differ only in the orientation of the OH group and have comparable stabilities in aqueous media. The present study was performed considering only the I conformer, but one would expect similar results if the II conformer is considered. The same three stable conformers of tyrosine (I, II and III) in gas phase have also been reported by Zhang *et al.* [52].

The optimized structure of the reactant complex of *cis* O6-MeG with a phenol molecule and those of the reactant complexes of *cis* O6-MeG with the three conformers I, II, III of tyrosine, denoted as RC1, RC2, RC3 and RC4 respectively, at the B3LYP/6-31G(d,p) level of theory in gas phase are presented in Fig. 2. Values of some important geometrical parameters of the four complexes are also given in this figure. According to the ZPE-corrected total energies obtained at the MP2/AUG-cc-pVDZ level of theory, RC3 and RC4 are less stable than RC2 in aqueous media by 1.7 and $5.6 \text{ kcal mol}^{-1}$ respectively (Fig. 2). The complexes RC2 and RC3 are stabilized by two hydrogen bonds each, i.e. a strong hydrogen bond between the N1 atom of *cis* O6-MeG and the H14 atom of the hydroxyl group of tyrosine and a weak hydrogen bond between the H2' atom of the amino group of *cis* O6-MeG and the O15 atom of the hydroxyl group of tyrosine in each case. However, RC4 is stabilized by a single hydrogen bond between the N1 atom O6-MeG and the H14 atom of the hydroxyl group of tyrosine. The N1H14 distances in RC2, RC3 and RC4 are 1.822, 1.822, 1.866 \AA while the H2'O15 distances in the three complexes are 2.183, 2.186, 2.757 \AA respectively (Fig. 2). As RC2 is most stable among the three reactant complexes, reactions between *cis* O6-MeG and tyrosine were considered to be initiated from it.

Repair of O6-methylguanine to guanine

We studied the mechanism of repair of O6-MeG to guanine by tyrosine starting with the reactant complex RC2. Details of the reaction involving the reactant complex RC2, transition states TS1 and TS2, intermediate complex IC1 and product complex PC1 are shown in Fig. 3. Since this reaction mainly involves the phenol moiety of tyrosine, the reaction was also studied considering only a phenol molecule in place of tyrosine, and the results thus obtained are presented in Fig. 4. The reactions shown in both the Figs. 3 and 4 involve two steps each. In the first step of each of these reactions, the N1 site of O6-MeG gets protonated as the H14 proton leaves the hydroxyl group of tyrosine and gets associated with it. In the second step of each of the reactions (Figs. 3, 4), the methyl group of O6-MeG gets detached from the O6 site of guanine and gets attached to the O15 site of the phenolate moiety. The ZPE-corrected barrier and released energies and net CHelpG charges (in the unit of magnitude of electronic charges) obtained at the MP2/AUG-cc-pVDZ level of theory in aqueous media using the geometries optimized at the B3LYP/6-31G(d,p) level of theory in gas phase along with certain optimized geometrical parameters are shown in Fig. 3. The ZPE-corrected barrier and released energies and the corresponding Gibbs energy changes obtained at the

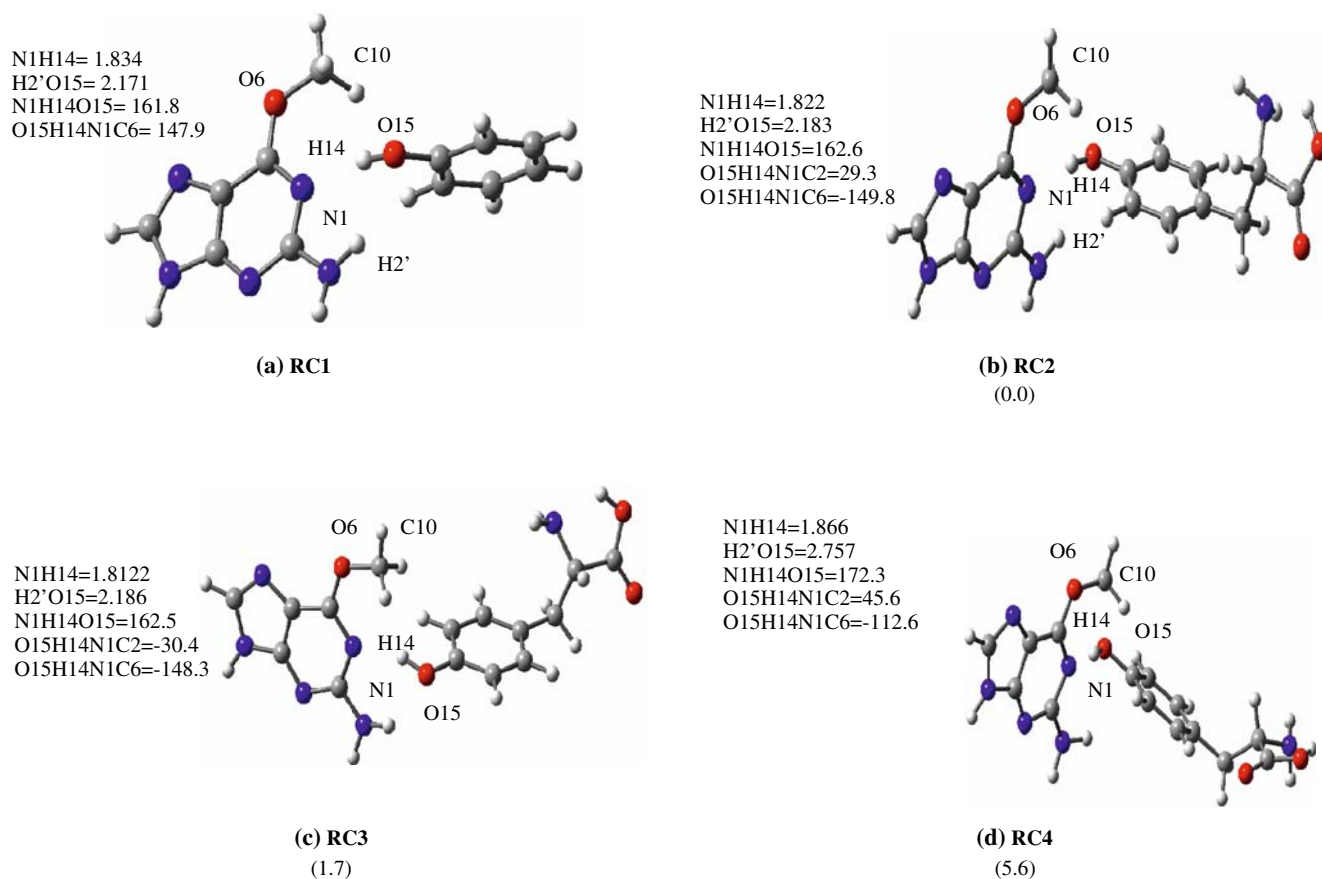


Fig. 2 Structures of reactant complexes RC1, RC2, RC3 and RC4 of *cis* O6-MeG with (a) Phenol, (b) TyrI, (c) TyrII and (d) TyrIII. Relative ZPE-corrected total energies (kcal mol^{-1}) of RC2, RC3 and RC4 obtained at the MP2/AUG-cc-pVDZ level of theory in aqueous

media using the geometries optimized at the B3LYP/6-31G(d,p) level in gas phase are given with respect to that of RC2. Atomic numbering scheme and some geometrical parameters optimized at the B3LYP/6-31G(d,p) level in gas phase (\AA , degree) are given

different levels of theory in gas phase and aqueous media are presented in Table 1.

In going from RC2 to TS1, the H14 proton of tyrosine leaves the hydroxyl group attached to the benzene ring of tyrosine and moves near the N1 atom of *cis* O6-MeG (Fig. 3). The N1H14 distance at TS1 is 1.360 \AA and so the corresponding bond is not yet formed. The intermediate complex (IC1) is formed when the H14 proton gets bonded to the N1 atom of O6-MeG. In the second step of the reaction, the methyl group moves from the O6 position of *cis* O6-MeG towards the O15 atom of the phenolate moiety of tyrosine. At TS2, the C10 atom of the methyl group is located between the O6 and O15 atoms, the O6C10 and O15C10 distances being 1.977 and 2.104 \AA respectively. After TS2, the product complex PC1 is formed. In the product complex PC1 (Fig. 3), guanine is recovered from O6-MeG while tyrosine is converted to O-methyl tyrosine. At IC1, the CHelpG charges associated with the protonated O6-MeG and deprotonated tyrosine moieties were found to be 0.89 and -0.89 that are in conformity with the cationic and anionic nature of the two species respectively.

media using the geometries optimized at the B3LYP/6-31G(d,p) level in gas phase are given with respect to that of RC2. Atomic numbering scheme and some geometrical parameters optimized at the B3LYP/6-31G(d,p) level in gas phase (\AA , degree) are given

The calculated ZPE-corrected barrier energies (ΔE^b) and the corresponding Gibbs energy changes ΔG^b involved in the reaction of O6-MeG with tyrosine (Table 1) reveal the following information. At the first step of the reaction, the gas phase barrier energy (ΔE_1^b) and the corresponding Gibbs energy change (ΔG_1^b) at the B3LYP/6-31G(d,p) level of theory were found to be 21.5 and 21.0 kcal mol^{-1} respectively, the corresponding values obtained at the B3LYP/AUG-cc-pVDZ level being 24.1 and 23.6 kcal mol^{-1} (Table 1). The ΔE_1^b and ΔG_1^b values at the MP2/AUG-cc-pVDZ level of theory in gas phase were also found to be similar to those obtained by the corresponding B3LYP calculations (Table 1). In going from gas phase to aqueous media, according to the B3LYP calculations, the values of ΔE_1^b and ΔG_1^b are somewhat reduced except in one case where there is a small increase, while according to the corresponding MP2 calculations the values of these energies are appreciably increased. We should consider the MP2 results to be more reliable than the corresponding B3LYP results, in view of a better electron correlation treatment in the former case than in the latter. At the second step of the reaction (Fig. 3), the

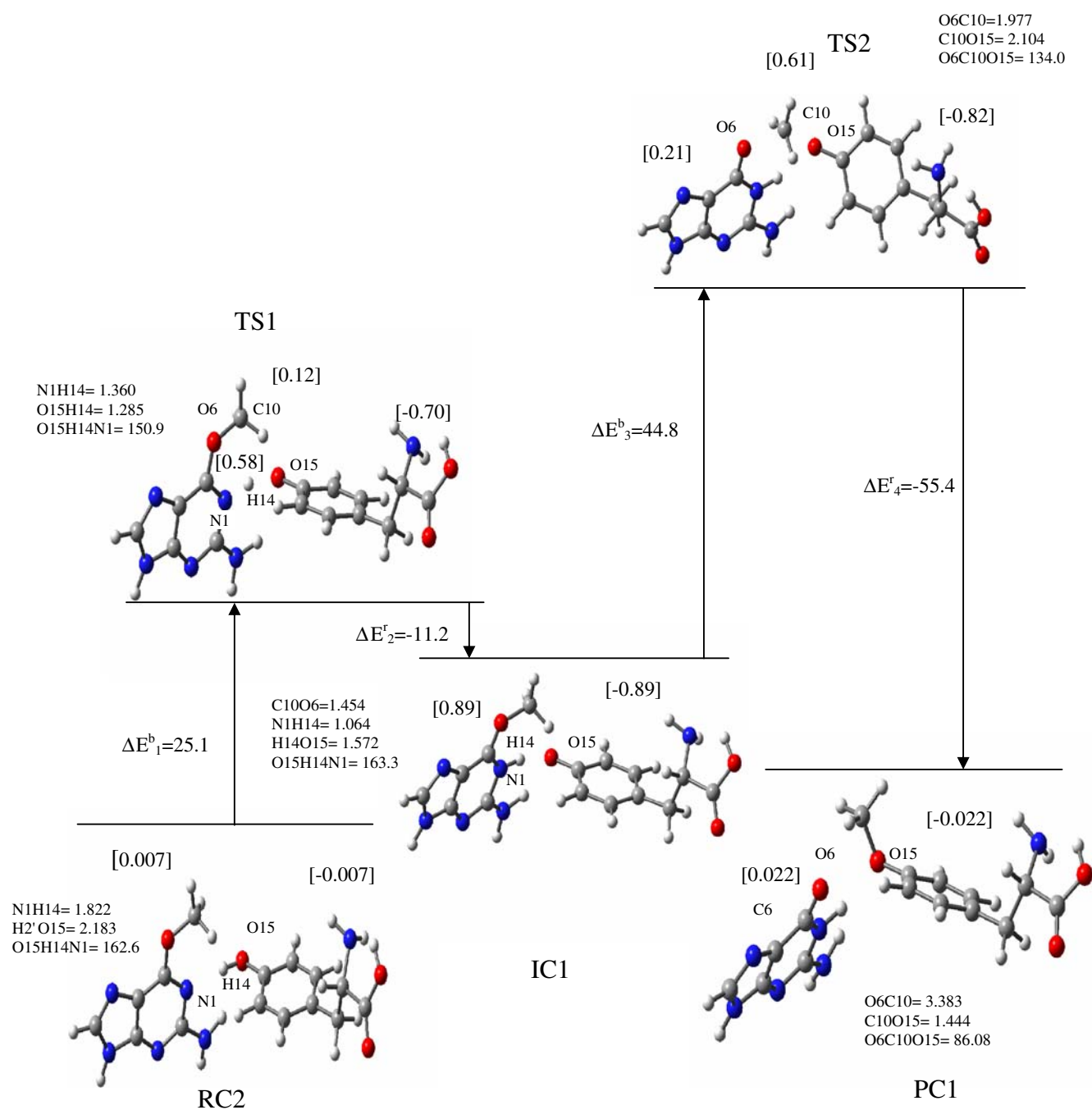


Fig. 3 Mechanism of repair of *cis* O6-MeG due to its reaction with the most stable conformer of tyrosine (TyrI). ZPE-corrected barrier (ΔE^b) and released (ΔE^r) energies (kcal mol^{-1}) and net CHelpG charges obtained at the MP2/AUG-cc-pVDZ level of theory in

aqueous media, and certain optimized geometrical parameters (\AA , degree) obtained at the B3LYP/6-31G(d,p) level of theory in gas phase are given

ZPE-corrected barrier energies (ΔE_3^b) and the corresponding Gibbs energy changes (ΔG_3^b) at the B3LYP/6-31G(d,p) and B3LYP/AUG-cc-pVDZ levels of theory in gas phase were found to lie in the range 41.0–43.5 kcal mol^{-1} . The values of ΔE_3^b and ΔG_3^b at the MP2/AUG-cc-pVDZ levels of theory in gas phase were found to be 43.9 and 45.4 kcal mol^{-1} respectively. In going from gas phase to aqueous media at the different

levels of theory, the values of ΔE_3^b and ΔG_3^b are changed only slightly. The ZPE-corrected barrier and Gibbs energies (ΔE_3^b and ΔG_3^b) that have values around 40 kcal mol^{-1} or more are too large to be overcome in biological media. Therefore, such reaction steps would not occur.

The results discussed above (Fig. 3, Table 1) show that it is the phenolic part of tyrosine that is involved in the repair

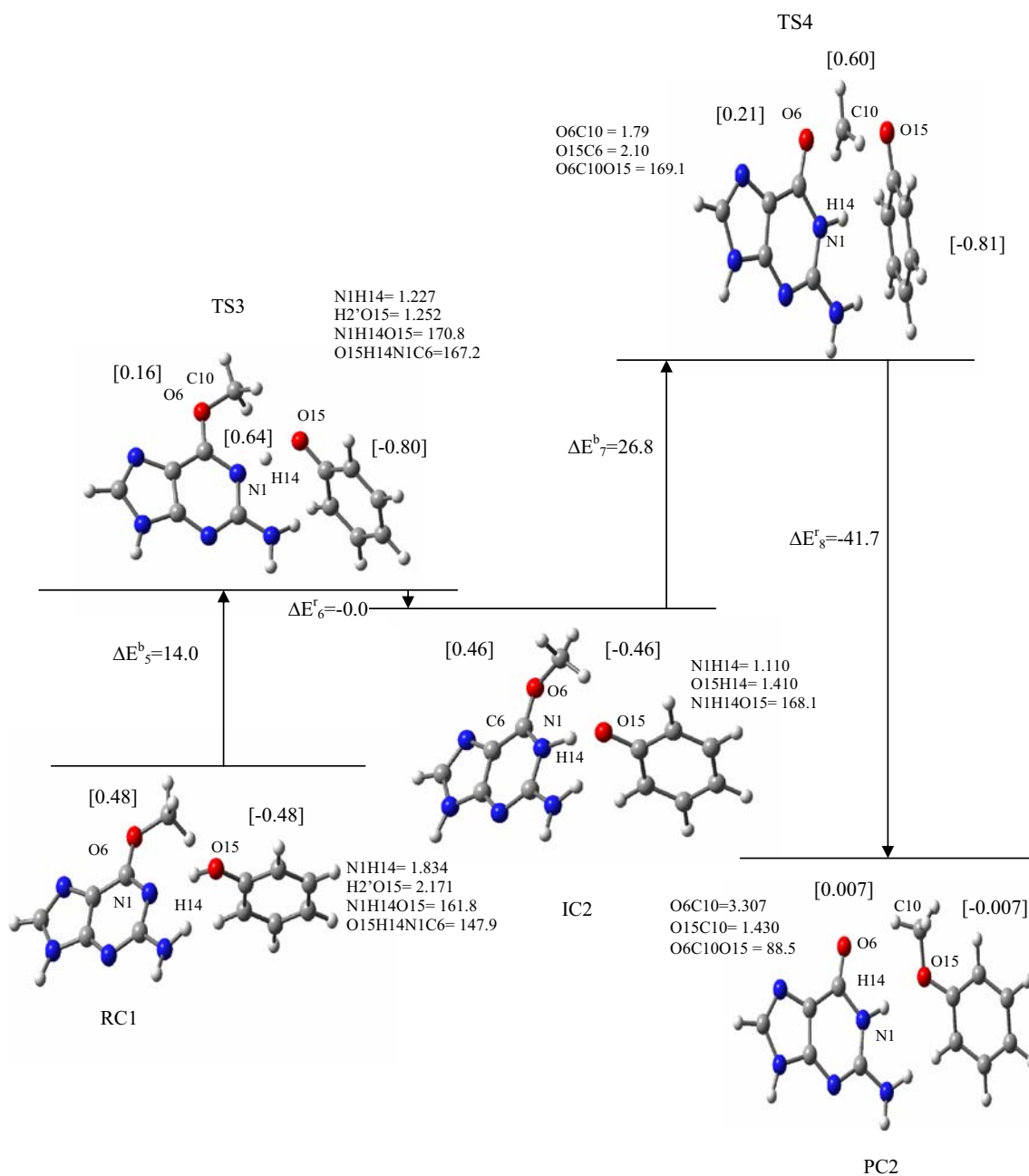


Fig. 4 Mechanism of repair of *cis* O6-MeG due to its reaction with phenol. ZPE-corrected barrier (ΔE^b) and released (ΔE^r) energies (kcal mol⁻¹) and net CHelpG charges obtained at the MP2/AUG-cc-pVDZ

level of theory in aqueous media, and certain optimized geometrical parameters (Å, degree) obtained at the B3LYP/6-31G(d,p) level of theory in gas phase are given

reaction of O6-MeG. In order to evaluate qualitatively the role of the chain attached to the phenol moiety of tyrosine, the repair reaction was also studied considering only a phenol molecule in place of tyrosine. The results thus obtained are presented in Fig. 4 and Table 2. The reactant complex RC1, transition states TS3 and TS4, intermediate complex IC2 and product complex PC2 involved in the repair of *cis* O6-MeG to guanine by a phenol molecule at the B3LYP/6-31G(d,p) level of theory in gas phase along with certain optimized geometrical parameters are shown in

Fig. 4. The ZPE-corrected barrier and released energies and net CHelpG charges obtained at the MP2/AUG-cc-pVDZ level of theory in aqueous media for this system are also given in Fig. 4. The ZPE-corrected barrier and released energies and the corresponding Gibbs energy changes in the reaction of O6-MeG with phenol (Fig. 4) obtained at the different levels of theory in gas phase and aqueous media are presented in Table 2.

The values of the ZPE-corrected barrier energy (ΔE_5^b) for the first step of the reaction (Fig. 4) obtained at the

Table 1 ZPE-corrected barrier (ΔE^b) and released (ΔE^r) energies and the corresponding Gibbs energy changes ΔG^b and ΔG^r respectively (kcal mol⁻¹) involved in the reaction of O6-MeG with tyrosine obtained at different levels of theory in gas phase and aqueous media^a

Barrier, released energies and corresponding Gibbs energy changes ^b	Level of theory ^c		
	B3LYP/6-31G(d,p)	B3LYP/AUG-cc-pVDZ	MP2/AUG-cc-pVDZ
ΔE_1^b	21.5 (22.9)	21.0 (18.6)	22.1(25.1)
ΔG_1^b	24.1 (22.3)	23.6 (21.2)	23.7(27.7)
ΔE_2^r	-4.1 (-9.6)	-5.4 (-5.8)	-4.4(-11.2)
ΔG_2^r	-5.0 (-6.9)	-5.9 (-6.8)	-4.4(-12.2)
ΔE_3^b	43.5 (43.8)	42.9 (41.3)	45.4(44.8)
ΔG_3^b	42.1 (41.9)	41.0 (39.8)	43.9(43.4)
ΔE_4^r	-59.7 (-61.9)	-57.4(-59.7)	-61.9(-55.4)
ΔG_4^r	-60.4 (-62.7)	-58.2(-60.4)	-62.6(-56.1)

^a Energies obtained in aqueous media are given in parentheses

^b See Fig. 4 for definition of the energies

^c Single point energy calculations were performed at the B3LYP/AUG-cc-pVDZ and MP2/AUG-cc-pVDZ levels employing the geometries optimized at the B3LYP/6-31G(d,p) level. In aqueous media, single point energy calculations were performed using the IEF-PCM

B3LYP/6-31G(d,p), B3LYP/AUG-cc-pVDZ and MP2/AUG-cc-pVDZ levels of theory in gas phase were found to be 19.2, 17.4 and 15.8 kcal mol⁻¹ respectively. The Gibbs energy changes (ΔG_5^b) for this reaction step were found to be larger than the corresponding ΔE_5^b values by ~ 2.1 kcal mol⁻¹ each (Table 2). In going from gas phase to aqueous media at the different levels of theory, ΔE_5^b and ΔG_5^b were reduced on the average by ~ 1.6 kcal mol⁻¹ (Table 2). For the second step of the reaction (Fig. 4), the ZPE-corrected barrier energies (ΔE_7^b) were found to be 35.7, 32.9 and 29.9 kcalmol⁻¹ at the B3LYP/6-31G(d,p), B3LYP/AUG-cc-pVDZ and MP2/AUG-cc-pVDZ levels of theory in gas phase respectively while the corresponding Gibbs energy changes ΔG_7^b were found to be ~ 2.1 kcal mol⁻¹ larger than ΔE_7^b .

In going from gas phase to aqueous media, ΔE_7^b and ΔG_7^b were found to be reduced on the average by ~ 3.2 kcal mol⁻¹ at the different levels of theory (Table 2). A comparison of the barrier energies and Gibbs free energies involved in the reaction of O6-MeG with tyrosine or phenol (Tables 1, 2) shows that the chain attached to the phenol moiety in tyrosine increases the barrier energies and Gibbs energy changes significantly.

We may compare the present results with those obtained for the repair of O6-MeG to guanine by cysteine in the absence or presence of histidine [35, 53]. There are two differences between the results obtained in the two cases: (i) While there is a single energy barrier when the repair is accomplished with cysteine in the absence or presence of histidine, there are

Table 2 ZPE-corrected barrier (ΔE^b) and released (ΔE^r) energies and the corresponding Gibbs energy changes ΔG^b and ΔG^r respectively (kcal mol⁻¹) involved in the reaction of O6-MeG with phenol molecule obtained at different levels of theory in gas phase and aqueous media^a

Barrier, released energies and corresponding Gibbs energy changes ^b	Level of theory ^c		
	B3LYP/6-31G(d,p) pVDZ	B3LYP/AUG-cc-pVDZ	MP2/AUG-cc-
ΔE_5^b	19.2 (17.8)	17.4 (15.9)	15.8(14.0)
ΔG_5^b	21.4 (19.9)	19.6 (18.1)	17.9(16.2)
ΔE_6^r	-2.8 (-4.1)	-1.8 (-3.2)	-1.5 (-0.0)
ΔG_6^r	-5.7 (-7.0)	-4.7 (-6.2)	-1.5 (-2.9)
ΔE_7^b	35.7 (32.8)	32.9 (29.3)	29.9 (26.8)
ΔG_7^b	37.8 (34.9)	35.0 (31.4)	31.9 (28.9)
ΔE_8^r	-52.3 (-49.5)	-49.0 (-45.5)	46.1 (-41.7)
ΔG_8^r	-54.0 (-51.2)	-50.7(-47.2)	-47.8 (-43.5)

^a Energies obtained in aqueous media are given in parentheses.

^b See Fig. 3 for definition of the energies.

^c Single point energy calculations were performed at the B3LYP/AUG-cc-pVDZ and MP2/AUG-cc-pVDZ levels employing the geometries optimized at the B3LYP/6-31G(d,p) level. In aqueous media, single point energy calculations were performed using the IEF-PCM.

two energy barriers when the repair is effected with tyrosine, and (ii) In the work of Georigeva and Himo [35], the barrier energy for the repair of O6-MeG to guanine by cysteine in the presence of histidine was found to be 18.2 kcal mol⁻¹ when the cluster model was considered while it was found to be 21.2 kcal mol⁻¹ when a homogeneous surrounding model was considered. In another work, the ZPE-corrected barrier energy obtained by a single point energy calculation at the MP2/6-31+G(d) level in aqueous media using the geometry optimized at the B3LYP/6-31+G(d) level was found to be 29.2 kcal mol⁻¹ [53]. In the case of tyrosine, according to the present work, the corresponding reaction can be effected by overcoming two barriers, one with energy 25.1 kcal mol⁻¹ and the other with energy 44.8 kcal mol⁻¹ as obtained by single point energy MP2/AUG-cc-pVDZ calculations in aqueous media using the geometries optimized at the B3LYP/6-31G(d,p) level in gas phase. In view of the large barrier energies, it appears that the repair of *cis* O6-MeG to guanine by tyrosine would be highly improbable. Thus it appears that only the HTH model would be feasible for the repair reaction in question, while the WHTH model would practically be inoperative.

Conclusions

The present study leads us to the following conclusions:

1. Tyrosine can repair O6-MeG to guanine by a two-step reaction, the first barrier energy being appreciably less than the second one. Further, this reaction mainly involves the phenol moiety of tyrosine.
2. There are two differences between the repair reactions of O6-MeG to guanine accomplished with cysteine, in the presence or absence of histidine, or with tyrosine. First, in the case of cysteine, the reaction involves a single step while in the case of tyrosine, the reaction involves two steps. Second, the barrier energy in the case of cysteine is much less than the second barrier energy in the case of tyrosine.
3. On the basis of barrier energies, it appears that the repair of *cis* O6-MeG to guanine by tyrosine would be highly improbable. In other words, it appears that only the HTH model would be feasible for the repair of *cis* O6-MeG to guanine, while the WHTH model would be practically inoperative.

Acknowledgments The authors are thankful to the Council of Scientific and Industrial Research (New Delhi) and the University Grants Commission (New Delhi) for financial support.

References

1. O'Brien P (2006) Chem Rev 106:302–323
2. Simons J (2006) Acc Chem Res 39:772–779
3. Burrows CJ, Muller JG (1998) Chem Rev 98:1109–1151
4. Halliwell B (1999) Mutat Res 443:37–52
5. Wyatt MD, Pittman DL (2006) Chem Res Toxicol 19:1580–1594
6. Jena NR, Mishra PC (2006) J Comput Chem 28:1321–1335
7. Jena NR, Mishra PC (2005) J Phys Chem B 109:14205–14218
8. Shukla PK, Mishra PC (2008) J Phys Chem B 112:4779–4789
9. Shukla MK, Mishra PC (1996) J Mol Struct 377:247–259
10. Mishina Y, Duguid EM, He C (2006) Chem Rev 106:215–232
11. Neeley WL, Essigmann JM (2006) Chem Res Toxicol 19:491–505
12. Bignami M, O' Driscoll M, Aquilina G, Karran P (2000) Mutat Res 462:71–82
13. Loechler EL et al (1984) Proc Natl Acad Sci (U.S.A.) 81:6271–6275
14. Samson L (1992) Mol Microbiol 6:825–831
15. Pegg AE, Dolan ME, Moschel RC (1995) Prog Nucl Acid Res Mol Biol 51:167–223
16. Mitra S, Kaina B (1993) Prog Nucl Acid Res Mol Biol 44:109–142
17. Rydberg B, Lindahl T (1982) EMBO J 1:211–216
18. Beranek DT (1990) Mutat Res 231:11–30
19. Kyrtopoulos SA, Anderson LM, Chhabra SK (1997) Cancer Detect Prev 21:391–405
20. Tubbs JL, Pegg AE, Tainer JA (2007) DNA Repair 6:1100–1115
21. Gerson SL, Liu L, Phillips WP, Zaidi NH, Heist A, Markowitz S, Wilson JKV (1994) Proc Am Assn Cancer Res 35:699–700
22. Dolan ME (1997) Adv Drug Delivery Reviews 26:105–118
23. Dolan ME, Pegg AE (1997) Clin Cancer Res 3:837–847
24. Rutledge LR, Durst HF, Wetmore SD (2008) Phys Chem Chem Phys 10:2801–2812
25. Rutledge LR, Wetmore SD (2008) J Chem Theory Comput 4:1768–1780
26. Rutledge LR, Campbell-Verduyn LS, Wetmore SD (2007) Chem Phys Lett 444:167–175
27. Pegg AE, Fang Q, Loktionova NA (2007) DNA Repair 6:1071–1078
28. Tubbs JL, Pegg AE, Tainer JA (2007) DNA Repair 6:1071–1078
29. Gerson SL (2002) J Clin Oncol 20:2388–2399
30. Fang Q, Gerson SL (2006) Clin Cancer Res 12:308–316
31. Pegg AE, Dolan ME, Moschel RC (1995) Prog Nucl Acid Res Mol Biol 51:167–223
32. Mishra SK, Mishra PC (2002) J Comput Chem 23:530–540
33. Kumar A, Mishra PC, Suhai S (2006) J Phys Chem A 110:7719–7727
34. Daniels DS, Woo TT, Luu KX, Noll DM, Clarke ND, Pegg AE, Tainer JA (2004) Nat Struct Mol Biol 11:714–720
35. Georgieva P, Himo F (2008) Chem Phys Lett 463:214–218
36. Goodtzova K, Kanugula S, Edara S, Pegg AE (1998) Biochem 37:12489–12495
37. Becke AD (1993) J Chem Phys 98:5648–5652
38. Lee C, Yang W, Parr RG (1998) Phys Rev B 37:785–789
39. Hariharan PC, Pople JA (1972) Chem Phys Lett 66:217–219
40. Møller C, Plesset MS (1934) Phys Rev 46:618–622
41. Frisch MJ, Head-Gordon M, Pople JA (1990) Chem Phys Lett 166:275–280
42. Woon DE, Dunning TH Jr (1993) J Chem Phys 98:1358–1371
43. Cancès MT, Mennucci B, Tomasi J (1997) Chem Phys 107:3032–3036
44. Cossi M, Barone V, Mennucci B, Tomasi J (1998) J Chem Phys Lett 286:253–263
45. Mennucci B, Tomasi J (1997) J Chem Phys 106:5151–5158
46. Tomasi J, Mennucci B, Cancès EJ (1999) Mol Struct (Theochem) 464:211–226

47. Breneman CM, Wiberg KB (1990) *J Comput Chem* 11:361–373
48. Frisch MJ, Trucks GW, Schlegel HB, Scuseria GE, Robb MA, Cheeseman JR, Zakrzewski VG, Montgomery JA Jr, Stratmann RE, Burant JC, Dapprich S, Millam JM, Daniels AD, Kudin KN, Strain MC, Farkas O, Tomasi J, Barone V, Cossi M, Cammi R, Mennucci B, Pomelli C, Adamo C, Clifford S, Ochterski J, Petersson GA, Ayala PY, Cui Q, Morokuma K, Rega N, Salvador P, Dannenberg JJ, Malick DK, Rabuck AD, Raghavachari K, Foresman JB, Cioslowski J, Ortiz JV, Baboul AG, Stefanov BB, Liu G, Liashenko A, Piskorz P, Komaromi I, Gomperts R, Martin RL, Fox DJ, Keith T, Al-Laham MA, Peng CY, Nanayakkara A, Challacombe M, Gill PMW, Johnson B, Chen W, Wong MW, Andres JL, Gonzalez C, Head-Gordon M, Replogle ES, Pople JA (2001) *Gaussian 98*, Rev A.11.2. Gaussian Inc, Pittsburgh PA
49. Frisch AE, Dennington RD, Keith TA, Neilsen AB, Holder AJ (2003) *GaussView*, Rev 3.9. Gaussian Inc, Pittsburgh PA
50. Parthasarathy R, Fridley SM (1986) *Carcinogenesis* 7:221–227
51. Pedersen LG, Darden TA, Deerfield DW II, Anderson MW, Hoel DG (1988) *Carcinogenesis* 9:1553–1562
52. Zhang M, Huang Z, Lin Z (2005) *J Chem Phys* 122:134313
53. Shukla PK, Mishra PC (in press)